A NEW TECHNIQUE FOR MEASURING THE BREAKTHROUGH CAPILLARY PRESSURE

Jonathan D. Smith, Ioannis Chatzis* and Marios A. Ioannidis
Porous Media Research Institute
Department of Chemical Engineering, University of Waterloo, Canada

ABSTRACT

The breakthrough capillary pressure is an important macroscopic property of porous media that is used to predict permeability and to correlate capillary pressure curves. It is normally determined using the porous plate method, where the non-wetting phase is introduced into the medium in increasing steps of pressure until it establishes a continuous pathway through the sample. In mercury porosimetry, breakthrough capillary pressure is identified as the pressure corresponding to about 10-20 % nonwetting phase saturation or the point of inflection in the drainage capillary pressure curve. A new method of measuring the breakthrough capillary pressure has been developed, involving a constant rate injection process as opposed to using incremental steps of constant pressure. The scope of this paper is to report the accuracy and reliability of the new technique in measuring the breakthrough capillary pressure by reporting test results on transparent micromodels and Berea sandstone core samples. In this study, air and mercury were used as the non-wetting phase while water (or brine, in the case of core samples) was the wetting phase. Constant rate injection was provided by means of a syringe pump, using water to displace a slug of either air or mercury in a tube connected to the porous medium at rates of about 1.8×10^{-2} cm^3/min. Pressure was measured at the sample inlet using a pressure transducer and data were recorded using a data acquisition system. The injection pressure-versus-time plot reveals the highest pressure established in such a test, which is identified as the breakthrough capillary pressure. It was concluded that the new test enables the determination of the breakthrough capillary pressure in micromodels with excellent accuracy. The new test was also validated for sandstone and carbonate core samples. The pore volume fraction of wetting phase displaced at the condition of gas breakthrough appears to correlate with the structure of the porous medium. The more homogeneous the sample is, the greater the fraction of wetting phase that is produced at the breakthrough capillary pressure.

INTRODUCTION

In the literature of immiscible displacements in porous media, the terms “breakthrough capillary pressure”, “threshold pressure”, “entry pressure” and “bubbling pressure” are frequently encountered. It has been observed, for example, that in order to make a nonwetting phase, such as air, flow through a porous medium saturated with brine, the applied capillary pressure on the air side has to exceed a critical limiting value, P_c^o, at which air can flow through the medium (i.e., can break through and emerge as bubbles

from the outlet face of the sample). The pore channels in the medium used by the air to break through the sample are made up of pore sizes greater than or equal to the pore size D_e^o, defined by the following equation,

$$P_c^o = \frac{4\sigma \cos\theta}{D_e^o} \quad [1]$$

where σ is the surface tension, θ is the contact angle and D_e^o is the (equivalent) diameter of a capillary tube which requires the same capillary pressure, P_c^o for penetration as that measured at breakthrough in the porous medium. The value of D_e^o calculated using Equation [1] is the minimum capillary size that is necessary for the non-wetting phase to traverse in order to break through the medium. If the pore shapes are cylindrical, the value of D_e^o calculated through Equation [1] is the true minimum capillary diameter along the breakthrough pathway. For pore cross-sections other than circular, D_e^o is always less than the effective diameter that characterizes the minimum cross-sectional area in the breakthrough pathway.

The "breakthrough pressure", which is also called the "bubble pressure" or the "threshold pressure", does not correspond either to zero nonwetting phase saturation or to "the diameter of the largest pore on the exterior of the rock sample" as defined by Craig [1]. Its value (a) depends on the degree of rock wettability and the fluid-fluid interfacial tension, as pointed out by Craig [1], and (b) corresponds to penetrating an intermediate pore size. Using capillary networks with randomly distributed pores, the exact pore size corresponding to the breakthrough capillary pressure depends on numerous factors, including pore coordination number, the dimensionality of the pore network, the size distribution of pore bodies and throats, and their spatial correlation structure, as analyzed by Chatzis and Dullien [2,3], Ioannidis and Chatzis [10] and Ioannidis et al. [11]. The spatial correlation structure involving large pore throats connecting large pore bodies in network models of pore structure leads to lower percolation thresholds and lower non-wetting phase saturation at breakthrough [11]. The "entry pressure" for penetrating the largest pore of entry at the exterior of the sample is, in general, different from the breakthrough pressure. For porous media that have a very narrow distribution of entry capillary sizes, as is the case of a uniform packing of equal spheres, however, the breakthrough pressure is the same as the "entry pressure" defined by the largest pore of entry size on the exterior of the sample.

The breakthrough capillary pressure is an important macroscopic pore structure parameter that is used to predict absolute permeability and to collapse capillary pressure curves using the reduced capillary pressure curves concept (Chatzis and Dullien [3]). Experimentally, the breakthrough capillary pressure is usually measured by two methods: (1) the detection of gas bubbles emerging from the outlet face of the sample that is saturated with a wetting liquid (e.g., water) prior to the gas displacement test. This technique was employed by Macmullin and Muccini [4] and Thomas et al. [5]; and (2) the detection of breakthrough by electrical means using mercury (El-Sayed [6]). The

sample is originally evacuated and mercury is used as the nonwetting fluid, allowing only one face for injection and attaching an electrode to the opposite face of the core sample (Chatzis and Dullien [3]). The applied capillary pressure is increased using small pressure increment steps to allow for quasi-static equilibrium conditions. The detection of breakthrough by the latter method is extremely sensitive and the experimental procedure and apparatus are relatively simple. Use of this method has been made by Chatzis [7], employing a new design of a mercury porosimeter, and by Thompson et al. [8]. Details are also provided in the book of Dullien [9].

The primary objective of this paper is to report details of a new experimental technique for the measurement of the breakthrough capillary pressure which involves the injection of a slug of a nonwetting phase at constant injection rate and monitoring the pressure trace at the face of injection. Comparison of the measured values with those predicted by other techniques is also made and discussed.

EXPERIMENTAL ASPECTS

Breakthrough Pressure in Air Displacing Water Experiments

Two types of porous media were utilized in the evaluation of the constant rate injection test: brine-saturated Berea sandstone cores and water-saturated glass micromodels. The Berea cores were covered with epoxy along their length such that penetration entry/exit could occur at only the two end faces. The micromodels were of two varieties: capillary networks etched on glass plates and glass beads sintered between glass plates. For the etched micromodels, pore networks were engraved into glass plates using hydrofluoric acid. Two plates containing mirror images of an etched network pattern were then placed together and fused at high temperature to create a self-contained pore network. For the glass bead micromodels, a layer of glass beads four to ten beads (~0.3 cm) thick was "sandwiched" between two glass plates. The model was then placed into an oven at high temperature and sintered together, binding the plates and beads together but leaving sufficient space within to maintain a pore network of space. Glass slabs were used to seal the ends of the model and thick rubber strips were used to seal the sides by binding them with powerful adhesive. For both micromodel types, holes of approximately 0.2 cm diameter were drilled at opposite ends on the plate face to provide an inlet and outlet port.

The experimental layouts for both Berea core and glass micromodel tests were essentially the same. The set-up consisted of a syringe pump, a 2 psi differential pressure transducer and the porous medium being tested joined at a T-connection (see Figure 1a). Flexible, fluoropolymer tubing, $^{1}/_{8}$" in diameter, was used to connect the system. The tubing between the syringe pump and the pressure transducer was completely filled with water to provide pressure response. Once the syringe pump was started, water began to invade the length of tubing between the T-connection and the test medium, pushing a slug of air into it. Various steady flow rates could be selected on the pump, with the lowest (and default) being 1.79×10^{-2} cm^3/min. An extended length of tubing was used to connect the porous medium to the T-connection so that the water front displacing the air would never reach the medium itself. Furthermore, to prevent hydrostatic pressure effects, the tubing

was kept level with the transducer so that as water moved through the tubing, its elevation remained constant.

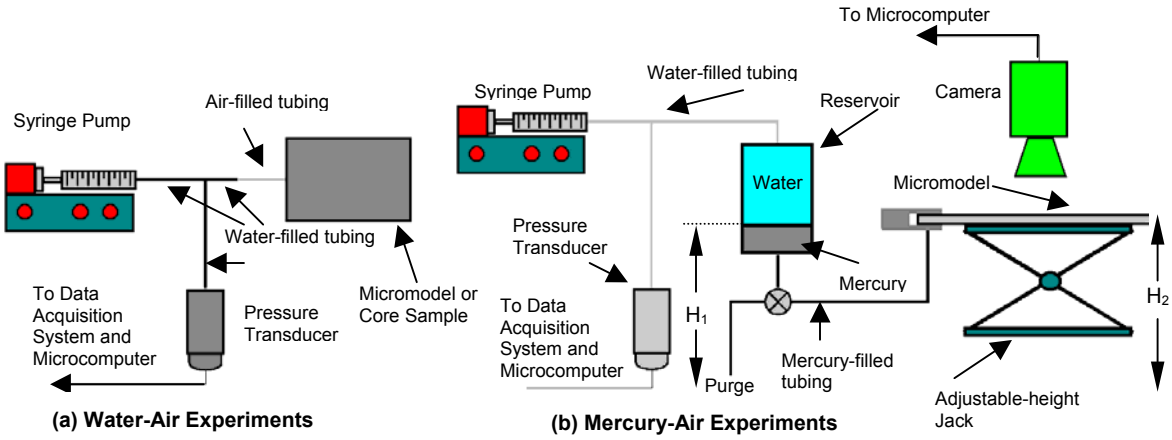

Figure 1: Experimental Apparatus Used for Core and Micromodel Experiments

Connections between the tubing and the micromodels were made using a threaded aluminium yoke and an o-ring tipped, ¼" NPT fitting with tube adapter. The fitting was tightened against the glass until the o-ring made a good seal. The cylindrical core samples were placed into a core holder with a welded tube fitting on each end. The apparatus was orientated both horizontally and vertically (such that injection occurred in the direction of gravity, allowing for non-preferential invasion of the pores by air). The small void space at the injection face (top) of the core holder was drained of brine using a short length of tubing at the outlet (bottom). This ensured air would not have to push brine through the core before beginning invasion. Since the void space at the outlet and attached tube were still filled with brine, breakthrough of air through the core was evident when bubbles of air appeared in the tube. To prevent pressure gradients due to hydrostatic effects, the tube was kept level with the outlet port during every experiment. A test tube was located at the end of the tubing and collected brine that was displaced from the core. After breakthrough was detected, the test tube was removed and weighed to provide a means to estimate non-wetting phase saturation at breakthrough. As the slug of air was pushed into the various porous media, the output from the pressure transducer (measuring inlet pressure) was recorded using a microcomputer and data acquisition system. This allowed for the construction of pressure vs. time plots and was an easy (non-visual) way to detect air breakthrough, since a sharp drop in pressure occurs at this point.

Mercury-Air Experiments

The procedure for the constant rate injection of mercury was similar to that used for the air-water system. A single, etched glass micromodel was used to evaluate the mercury test. Water-filled fluoropolymer tubing was used to connect the syringe pump, the pressure transducer and an elevated reservoir. The reservoir was filled with water on top of mercury, as shown in Figure 1b. Mercury displaced by water was allowed to exit the

reservoir outlet and was directed to the micromodel using flexible fluoropolymer tubing. A connection to the micromodel was made in a similar manner as detailed with the air-water experiments. The micromodel itself was placed on an adjustable-height jack, so that the height of the micromodel could be matched as close as possible to the height of mercury in the reservoir. The pressure transducer measured a pressure that was higher than the actual capillary pressure due to the height difference between the reservoir and the pressure transducer. This offset is shown as H_1in Figure 1b and was recorded before each experiment. The pressure measured by the transducer could also have been affected by a height difference, $H_2 - H_1$ (shown in Figure 1b), between the micromodel and the water-mercury interface in the reservoir. Assuming an accuracy of 1 mm in the levelling, the accuracy of the capillary pressure readings is about ±1.4 cm H_2O in this experiment. The pressure reading from the transducer was recorded using a microcomputer and a data acquisition system during the experiment. Furthermore, a video camera placed above the micromodel was used to video-record and take snap shots of the invasion process during the experiment. The video signal was sent directly to a microcomputer for storage and subsequent image processing. The general procedure is very similar to that adopted for rate-controlled porosimetry by Yuan and Swanson [13] in the APEX method.

Drainage Capillary Height Tests

To verify the values of breakthrough capillary pressure obtained for the micromodels, drainage capillary height tests were performed. In such a test, a water-filled tube was connected to a water-saturated micromodel. The other end of the tube was placed inside a large beaker of water. The micromodel was then placed vertically and had its elevation raised until it began to drain. Capillary pressure inside the model was taken to be the height difference between the lowest air-water interface seen in the micromodel and the level of water in the beaker. By increasing the height of the micromodel above the beaker, drainage is imposed and new capillary interfaces are established in the model. Once approximately 20 to 30 minutes passed (allowing the system to equilibrate), capillary drainage height measurements were made. In order to sample representative drainage capillary pressure values in the pathways invaded by the non-wetting phase front, this activity was repeated until the air-water interface reached the bottom of the micromodel.

RESULTS

Air Displacing Water Tests in Micromodels

Several micromodels were tested using constant rate injection. The air was observed to enter the media once the pressure exceeded the entry pressure of the largest pore at the face of injection. The results for the etched and glass bead micromodels are shown below in Table 1 and Table 2 respectively. The breakthrough pressure values determined from the test are compared to the results of drainage tests, as detailed previously in the procedure section. Figure 2 shows a typical pressure trace of micromodel 1 at an injection rate of 1.79×10^{-2} cm^3/min, implying a breakthrough pressure of approximately 14.0 cm H_2O. The points labelled ‘A’ to ‘E’ correspond to the same locations in the micromodel as the points similarly labelled in Figure 3. Of interest are the various

"peaks" and "valleys" on the graph, corresponding to pressure build-up at the non-wetting phase front and subsequent intrusion into larger size pores after the pressure exceeds the limiting value.

Table 1: Breakthrough Pressure Results for Etched Glass Micromodels

Model	Width	Length	Permeability	Breakthrough Pressure (cm Water)		Relative Difference
	cm	*cm*	*Darcy*	*Drainage Height*	*Const. Rate Injection*	*%*
1	5.0	16.4	333.0	15.0	14.0	6.67
2	3.4	11.0	24.3	54.0	52.5	2.78
3	7.6	12.1	137.8	24.7	23.3	5.67
4	6.3	13.7	31.4	20.3	19.0	6.40

Table 2: Breakthrough Pressure Results for Glass Bead Micromodels

Model	Width	Length	Permeability	Breakthrough Pressure (cm Water)		Relative Difference
	cm	*cm*	*Darcy*	*Drainage Height*	*Const. Rate Injection*	*%*
5	7.3	26.5	4.7	40.0	42.5	-6.25
6	4.8	19.4	13.9	22.5	22.8	-1.33
7	8.6	32.0	50.2	17.0	18.2	-7.06
8	9.5	29.3	31.0	18.0	19.2	-6.67

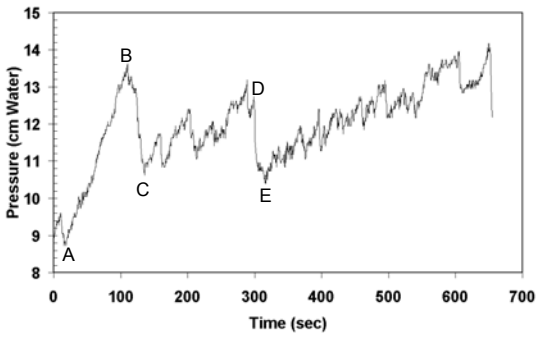

Figure 2: Typical Pressure Trace for Micromodel 1 (Air-Water)

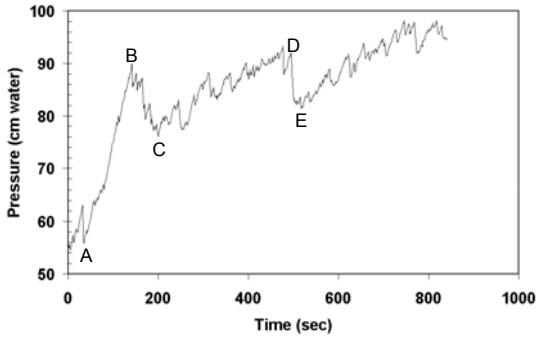

Figure 3: Typical Pressure Trace for Micromodel 1 (Mercury-Air)

Mercury-Air Tests in Micromodels

Micromodel 1 (etched) was used for the mercury experiments. Three different runs were performed, all yielding essentially the same results. Figure 3 shows a typical pressure trace, implying a breakthrough pressure of approximately 97 cm H_2O. As previously mentioned, points 'A' to 'E' are meant for use in comparing air-water and mercury-air pressures at the same locations in Micromodel 1. The end of the plot is the breakthrough point; it is not obvious (as in the case of Figure 2) because injection was ceased immediately after breakthrough to prevent mercury being ejected from the micromodel. In order to correct for the difference in surface tension between water and mercury, the breakthrough pressure is multiplied by $(\sigma_{W\text{-}A}\cdot\cos\theta_{W\text{-}A} / \sigma_{Hg\text{-}A}\cdot\cos\theta_{Hg\text{-}A})$. The surface tension

of mercury and water were taken as 485 and 72 dynes/cm, respectively. The accompanying mercury and water receding contact angles used were 35° and 0°. A resulting value of 17.6 cm H_2O was calculated, in comparison to 14.0 cm H_2O for the same model using the air-water system and 15.0 cm H_2O using the capillary drainage height test. Figure 4 shows snapshots of an experiment before and after mercury breakthrough. It was observed that mercury breaks through only a single pore at the exit end; this fact is obvious in the second part of Figure 4.

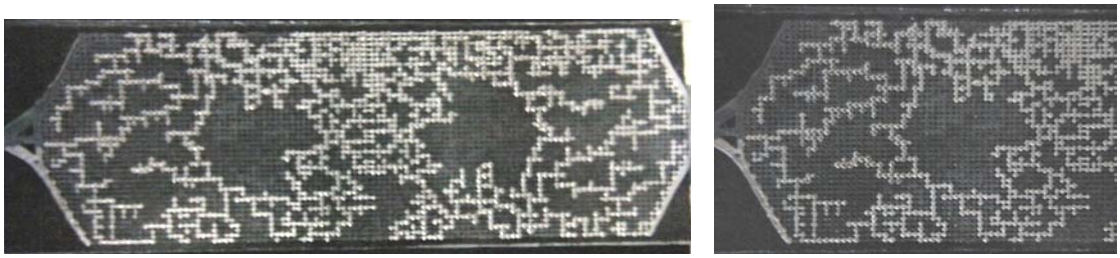

Figure 4: Mercury Injection into Micromodel 1 (Overall and Exit-Half Views)

Air-Water Displacement Tests in Berea Sandstone

The constant rate injection test was used to determine the breakthrough pressure of two different Berea sandstone cores. The results are shown below in Table 3, with the breakthrough pressure values being the typical results obtained over several runs. Core 1 was studied using both a horizontal and vertical orientation, whereas Core 2 was studied solely using a horizontal orientation. Figure 5 shows a typical result for Core 1 in the vertical position, implying a breakthrough pressure of approximately 88 cm H_2O. The typical non-wetting phase saturation at breakthrough, calculated using the weight of brine displaced during an experiment, was approximately 14.5%. Within twenty-four hours of the experiment shown in Figure 5, air was re-injected into the undisturbed core to study the secondary drainage characteristics, with the results shown in Figure 6. To provide a means for breakthrough pressure comparison, a section of Core 1 previously cut off was used for mercury porosimetry. The resulting saturation-capillary pressure curve is shown in Figure 7. Furthermore, the results were compared to permeability correlations from Chatzis [7] and Ioannidis and Chatzis [10]. In the correlation for sandstones, the breakthrough capillary pressure for the fluid pair of air-brine in Berea sandstones is given by

$$P_c^{o}{}_{(air\text{-}brine)} = 938.5 \cdot K^{-0.36} \qquad [2]$$

where K is permeability to brine in millidarcy and P_c^o is the breakthrough pressure in cm H_2O. In the correlation of Ioannidis and Chatzis [10] for Silurian carbonate core samples

$$P_c^{o}{}_{(air\text{-}brine)} = 257.5 \cdot K^{-0.34} \qquad [3]$$

where P_c^o and K have the units of cm H_2O and millidarcy respectively. Table 4 shows the corresponding values of breakthrough pressure based on the two correlations, in comparison to the values determined by constant rate air injection. Although the experimental values are not in good agreement with the correlation predictions, they are within the ± 50% range of Equation [2] at low pressures.

Table 3: Results of Constant Rate Air Injection for Berea Sandstone Cores

Core	Length	Diameter	Porosity	Brine Permeability	Breakthrough Pressure
	cm	*cm*		*mD*	*cm Water*
1	3.7	3.7	0.22	270	88
2	5.8	3.5	0.26	518	55

Table 4: Comparison of Results with Sandstone and Carbonate Core Correlations

Core	Permeability To Brine	Breakthrough Capillary Pressure (cm H_2O)		
		Berea Sandstone Correlation	Vuggy Carbonate Correlation	Air Injection
	mD	*Equation [2]*	*Equation [3]*	
1	270	125.1	38.4	88
2	518	98.9	30.8	55

DISCUSSION

Constant rate air injection has been shown to predict the breakthrough capillary pressure of micromodels accurately when compared to the drainage capillary height method, as seen in Tables 1 and 2. Experiments on micromodels using mercury as the non-wetting phase show relatively good agreement in terms of the value of breakthrough pressure and reveal similar 'structure' in the pressure trace, as seen when comparing Figures 2 and 3. It is obvious, however, that using mercury as the non-wetting phase takes significantly longer than air. This is easily explained by the fact that air must displace an incompressible wetting phase fluid, making it difficult to invade saturated areas that have been isolated by air pathways. Mercury is able to invade regions of trapped air much easier, resulting in a higher magnitude of non-wetting phase saturation and consequently a longer breakthrough time.

When applied to core samples, the accuracy of the air injection test can not be proven directly without using mercury porosimetry. Lai et al. [12] have shown that the drainage-capillary pressure curve obtained by mercury porosimetry is affected by the surface-to-volume ratio of the bulk sample (see Figure 8). Since the arbitrary nature of determining breakthrough pressure from saturation-capillary pressure curves at the point of inflection, as argued by Thomson et al. [8], is being questioned in our paper, unbiased comparison is not possible. Yet, as seen in Figure 7, the value of breakthrough capillary pressure as it has been traditionally determined lies somewhere between 6 and 8 psi, or 77 and 102 cm H_2O when surface tension and wetting angle are taken into account. The breakthrough pressure value determined by air injection was 88 cm H_2O, approximately half way

between the previously mentioned range. This represents a difference of only 14% either way if the actual breakthrough pressure was one of the extreme values.

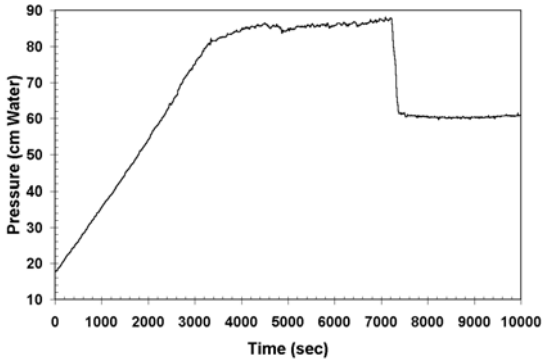

Figure 5: Typical Pressure Trace for Berea Core 1 (Vertical Orientation)

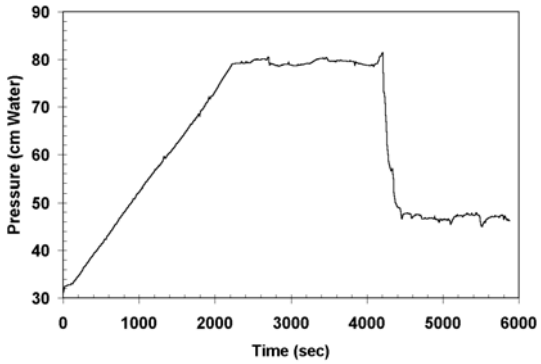

Figure 6: Pressure Trace Showing Secondary Drainage of Berea Core 1

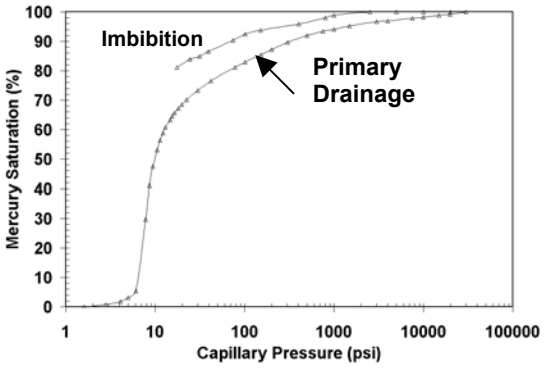

Figure 7: Mercury Porosimetry Results of Drainage and Imbibition for Berea Core 1

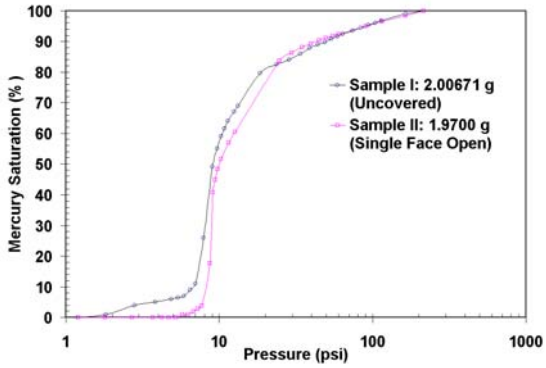

Figure 8: Porosimetry Results from Lai et al. [12]

Based on various experiments using horizontal and vertical core orientations, it appears that vertical core orientation is most accurate. Tests run on horizontal samples do not allow for non-preferential invasion, as air will invade the uppermost part in a brine-saturated core sample because of gravity effects. In vertical orientations of short cores the non-wetting phase samples the entire cross-section for pore invasion. Furthermore, tests run on horizontal samples tend to yield an unexplainable 'hump' or rise in pressure at the start of the experiment that is greater than the breakthrough pressure and not likely characteristic of the test media. Cores analysed in using a vertical orientation do not experience this rise in pressure, which essentially rules out viscous pressure drop as the cause. When using a vertical orientation, a slight error is incurred that is proportional to the length of the core. The non-wetting phase penetrates at a lower pressure than it would in a very short core because of hydrostatic pressure drop. This error in pressure is highest when the non-wetting phase first contacts the core at the top and is negligible just

before breakthrough, when air is near the bottom end of the core. Because Core 1 was only 3.7 cm long, the maximum error is 3.7 cm H_2O; since the maximum pressure during the tests occurred near breakthrough, hydrostatic effects are not of concern here.

At breakthrough in water-air experiments, snap off of the non-wetting phase takes place as pressure is suddenly released. For the mercury-air experiments, the pressure decreased only slightly (~ 3 – 4 cm H_2O) after mercury breakthrough before disconnection occurred, due to the incompressible nature of mercury. For the air-water system in the same micromodel, the pressure dropped almost to zero. Figure 5 shows that upon decompression of the air phase in the core experiment at breakthrough (time 7300 sec), the pressure drops nearly 30 cm H_2O before disconnection occurs, although this value tends to vary a great deal. Upon re-injecting air into a previously tested core containing residual air, the pressure tends to rise to a value lower than the breakthrough pressure during primary drainage (see Figure 6). The pressure is maintained for some time at that value before a second major breakthrough (time 4200 sec) occurs and decompression of the gas phase is experienced. Curiously, the pressure to which the air builds up during secondary drainage (~ 80 cm H_2O) corresponds to approximately the same pressure at which invasion first occurred into the saturated medium (as detected by brine production at the outlet). Note the similar shape in Figures 5 and 6, as well as the similarity in duration of the plateau region. During secondary drainage in mercury porosimetry, the reconnection of residual mercury was found to happen at a lower breakthrough pressure [7]. The results presented in Figure 6 are consistent with the notion that residual non-wetting phase helps in establishing a lower breakthrough pressure due to increased pore accessibility [7].

The sensitivity of air injection for use in determining the detailed internal structure of a core sample is limited. While sharp drops or increases in pressure can identify possible vuggs, or represent the build up of pressure at smaller pores followed by subsequent invasion into areas of larger pores, the magnitude of responses on the pressure trace is strongly affected by the overall volume of air being injected. Since air is a compressible fluid, a larger amount will result in a less sensitive test. Certainly, constant rate air injection is not able to reveal macroscopic and microscopic pore characteristics to the degree that the APEX method [13] can, a test method with which air injection shares many similarities. Although mercury would provide much better structural information, errors caused by hydrostatic pressure effects would likely render it useless when being used in a manner similar to that detailed earlier in this paper for media of comparable permeability.

Viscous pressure drop in media of low permeability ($K < 10$ mD) is a concern when considering the accuracy of constant rate injection. At the condition of non-wetting phase breakthrough, the effective permeability of the invaded space is a very small fraction of the absolute permeability, because the invaded pore space is poorly interconnected and the flow of non-wetting phase is controlled by a select small number of pores. The tendency of mercury to channel irregularly through small segments of pores followed by

areas of high interconnectivity is obvious in Figure 4. The largest single segment channelling mercury flow occurs at the exit end and contributes the majority of the viscous pressure drop experienced in the micromodel. A rough estimate of this pressure was calculated using the Hagen-Poiseuille equation, assuming a mercury viscosity of 1.6 cP, a flow rate of 1.79 x 10^{-2} cm^3/min and the single channel to be a cylindrical tube of length 3 cm (the approximate length of the segment). The diameter was taken to be the breakthrough diameter of the micromodel, calculated using Equation [1]. This results in a viscous pressure drop value of approximately 8.0 cm H_2O. If subtracted from the breakthrough pressure in the mercury-air system, it reduces the breakthrough capillary pressure value to 89.0 cm H_2O. When scaled to account for surface tension and contact angle, the corresponding air-water breakthrough pressure of 16.1 cm H_2O is in better agreement with the value of 14.0 cm H_2O from the air-water system. Using Darcy's Law for Berea Core 1 (K = 270 mD), a maximum viscous pressure drop of 0.46 cm H_2O using a flow rate of 1.79 x 10^{-2} cm^3/min. For cores of much lower permeability, viscous pressure drop could become a serious issue if testing is not accompanied by a sharp reduction in the air injection rate.

Of additional interest is the similarity between the correlations relating permeability to breakthrough pressure in various media. If a power law relationship is used to relate breakthrough capillary pressure to permeability, the data reported in Table 2 give a correlation of the form $P_c^o = 67.8 \cdot K^{0.36}$. The exponent on permeability is the same as that found in Equations [2] and [3]. This suggests an explicit, medium-independent relationship between permeability and breakthrough capillary pressure may exist. More theoretical and experimental work is required to elucidate the key reason for this similarity for porous media that have major differences in pore structure.

The results show that constant rate air injection as a means to determine breakthrough capillary pressure has promise. The test allows for the direct calculation of breakthrough pore diameter and reveals some, albeit limited, pore structure information. It is simple, fast and non-destructive, and holds potential for use in an expanded range of media not explored in this study.

CONCLUSIONS

- Constant rate air injection permits the determination of the breakthrough capillary pressure of glass micromodels with excellent accuracy.
- Constant rate air injection permits the determination of the breakthrough capillary pressure of brine-saturated sandstone cores accurately.
- The point of inflection in the drainage capillary pressure curve overestimates the breakthrough capillary pressure.
- The trace of the dynamic pressure measured during constant rate injection of the non-wetting phase reveals information about the pore structure. For mercury-air and air-water displacements in glass micromodels of capillary networks, the characteristics of the dynamic pressure with time at the face of injection are very similar.

ACKNOWLEDGEMENTS

The Natural Sciences and Engineering Research Council (NSERC) of Canada provided the financial support of this research and it is gratefully acknowledged.

REFERENCES

1. Craig, F.F., *The Reservoir Engineering Aspects of Waterflooding*, Monograph Series Volume 3, SPE of AIME, New York, (1971).
2. Chatzis, I. and F.A.L. Dullien, " Modelling Pore Structure by 2-D and 3-D Networks With Application to Sandstones", *J. Canadian Petroleum Technology*, (1977) **16**, 97.
3. Chatzis, I. and F.A.L. Dullien, "The Modelling of Mercury Porosimetry and the Relative Permeability of Mercury in Sandstones Using Percolation Theory", *International Chemical Engineering*, (1985) **25**, 1, p.p. 47-66.
4. MacMullin, R.B. and G.A. Muccini, "Characteristics of Porous Beds and Structures", *AIChE Journal*, (1956) **2**, 3, p.p. 393-403.
5. Thomas, L.K., D.L. Katz and M.R. Tek, "Threshold Pressure Phenomena in Porous Media", *SPE Journal*, (1968) **174**.
6. El-Sayed, M.S., *Investigation of Transport Phenomena and Pore Structure of Sandstone Samples*, Ph.D. Thesis, University of Waterloo, Waterloo ON, (1979).
7. Chatzis, I. *A Network Approach to Analyze and Model Capillary and Transport Phenomena in Porous Media*, Ph.D. Thesis, University of Waterloo, Waterloo ON, (1980).
8. Thompson, A.H., A.J. Katz and C.E. Krohn, "The Microgeometry and Transport Properties of Sedimentary Rock", *Advances in Physics*, (1987) **36**, 5, p.p. 625-694
9. Dullien, F.A.L., *Porous Media: Fluid Transport and Pore Structure*, 2nd Edition, Academic Press Inc., Toronto, (1992).
10. Ioannidis, M.A. and I. Chatzis, *A Dual-Network Model of Pore Structure for Vuggy Carbonates*, Paper No. 2009, 2000 International SCA Symposium, Oct. 18-22, Abu-Dabi, United Arab Emirates.
11. Ioannidis, M.A., I. Chatzis and E.A. Sudicky, "The Effect of Spatial Correlations on the Accessibility Characteristics of Three-Dimensional Cubic Networks as Related to Drainage Displacements in Porous Media", *Water Resources Research*, (1993) **29**, p.p. 1777-1785.
12. Lai, F., I.F. Macdonald, F.A.L. Dullien and I. Chatzis, *J. Colloid Interface Science.*, (1981) **84,** 362.
13. Yuan, H.H. and B.F. Swanson, "Resolving Pore-Space Characteristics by Rate Controlled Porosimetry", *SPE Formation Evaluation*, (1989) **4**, 1.